BLMP-1 promotes developmental cell death in *C. elegans* by timely repression of *ced-9*/*bcl-2* transcription

Hang-Shiang Jiang[1,†], Piya Ghose[2,3,†,*], Hsiao-Fen Han[1], Yun-Zhe Wu[1], Ya-Yin Tsai[1], Huang-Chin Lin[1], Wei-Chin Tseng[1], Jui-Ching Wu[4], Shai Shaham[2,*], and Yi-Chun Wu[1,5,6,*]

[1]Institute of Molecular and Cellular Biology, National Taiwan University, Taipei, Taiwan

[2]Laboratory of Developmental Genetics, The Rockefeller University, New York, NY 10065, USA

[3]Department of Biology, The University of Texas at Arlington, Arlington, TX 76019, USA

[4]Institute of Clinical Laboratory Sciences and Medical Biotechnology, College of Medicine, National Taiwan University, Taipei, Taiwan

[5]Department of Life Science, Center for Systems Biology, and Research Center for Developmental Biology and Regenerative Medicine, National Taiwan University, Taipei, Taiwan

[6]Institute of Atomic and Molecular Sciences, Academia Sinica, Taipei, Taiwan

[†]These authors contributed equally.

[*]Corresponding authors: Yi-Chun Wu, E-mail: yichun@ntu.edu.tw, Phone: +(886)-2-33662483, Fax: +(886)-2-33665248; Piya Ghose, E-mail: piya.ghose@uta.edu, Phone: (817) 272-7132; Shai Shaham, E-mail: shaham@rockefeller.edu, Phone: (212) 327-7126, Fax: (212) 327- 7129.

ABSTRACT

Programmed cell death (PCD) is a common cell fate in metazoan development. PCD effectors are extensively studied, but how they are temporally regulated is less understood. Here we report a mechanism controlling tail-spike cell death onset during *C. elegans* development. We show that the Zn-finger transcription factor BLMP-1/Blimp1, which controls larval development timing, also regulates embryonic tail-spike cell death initiation. BLMP-1 functions upstream of CED-9/BCL-2 and in parallel to DRE-1/FBXO11, another CED-9 and tail-spike cell death regulator. BLMP-1 expression is detected in the tail-spike cell shortly after the cell is born, and *blmp-1* mutations promote *ced-9*-dependent tail-spike cell survival. BLMP-1 binds *ced-9*/*bcl-2* gene regulatory sequences, and inhibits *ced-9* transcription just before cell-death onset. BLMP-1 and DRE-1 function together to regulate developmental timing, and their mammalian homologs regulate B-lymphocyte fate. Our results, therefore, identify roles for developmental timing genes in cell-death initiation, and suggest conservation of these functions.

INTRODUCTION

Programmed cell death (PCD) is fundamentally important for the development of multicellular organisms. PCD promotes tissue and organ morphogenesis, removes cells that are harmful or no longer needed, and controls cell number homeostasis (Suzanne and Steller, 2013). PCD effectors have been studied in detail in the context of developmental apoptosis (Fuchs and Steller, 2011), and to a lesser extent in non-apoptotic developmental cell culling (Kutscher and Shaham, 2017). Mechanisms that ensure precise temporal onset of specific PCD events during development are not well understood.

The nematode *C. elegans* provides an excellent setting for deciphering mechanisms of PCD initiation. The animal's invariant cell lineage, transparency, and reporter-transgene expression toolkit, combined with facile genetics, allow real-time visualization of reproducible cell death events, and rapid gene discovery (Conradt et al., 2016; Sulston and Horvitz, 1977; Sulston et al., 1983). During *C. elegans* hermaphrodite embryogenesis, 113 cells die by apoptosis, a highly conserved cell-autonomous PCD form (Conradt et al., 2016; Nagata, 2018; Suzanne and Steller, 2013). In most of these cells, transcriptional activation of *egl-1*, encoding a BH3-only protein, initiates cell demise. EGL-1/BH3-only binds to CED-9/BCL-2 (Conradt and Horvitz, 1998; Hengartner and Horvitz, 1994), thereby releasing CED-4/Apaf-1 from CED-9/CED-4 complexes in the outer mitochondrial membrane (del Peso et al., 2000; del Peso et al., 1998). CED-4/Apaf-1, in turn, translocates to perinuclear membranes, where it binds to and activates CED-3 caspase, leading to cell death (Chen et al., 2000; Yang et al., 1998; Yuan et al., 1993). While most *C. elegans* cells destined to die undergo PCD shortly after they are generated (10-30 min), a few live for several hours, and can differentiate and function before death ensues (Sulston and Horvitz, 1977; Sulston et al., 1983). This extended timeline provides a unique opportunity to dissect cell death initiation control (Abraham et al., 2007; Maurer et al., 2007).

The *C. elegans* tail-spike cell, which is required for embryonic tail formation (Ghose et al., 2018), is one such cell. During development, the cell, generated by the fusion of two adjacent lineally-homologous cells, extends a microtubule-laden process that associates with the hypodermis. Once the tail forms, the cell undergoes Compartmentalized Cell Elimination (CCE), in which three caspase-dependent programs drive degradation of the proximal process, cell body, and distal process, in that order (Ghose et al., 2018; Maurer et al., 2007) (Figure 1A). Unlike other dying cells, EGL-1 plays only a minor role in tail-spike cell death. Thus, cell death onset must be determined by other means. Previous studies revealed that *ced-3* transcription is induced within 30 minutes of tail-spike cell death initiation. While this

induction requires the homeodomain transcription factor PAL-1, this protein is constitutively expressed in the tail-spike cell, and cannot alone account for temporal control of cell death onset (Edgar et al., 2001; Maurer et al., 2007). DRE-1, an F-Box protein related to mammalian FBXO11, also controls tail-spike cell death, likely through ubiquitylation and degradation of CED-9/BCL-2 (Chiorazzi et al., 2013). Although DRE-1 was previously shown to control developmental timing in larva (Fielenbach et al., 2007), whether it exerts temporal control on tail-spike cell death has not been determined.

Here we report that the *C. elegans* protein BLMP-1, a Zn-finger transcription factor similar to mouse Blimp-1(Huang, 1994; Keller and Maniatis, 1991), is a key regulator of tail-spike cell death. *blmp-1* is expressed in the tail-spike cell and functions there for tail-spike cell demise. BLMP-1 protein binds to regulatory DNA sequences in the *ced-9* gene, and blocks *ced-9* transcription right before tail-spike cell death onset. This allows the tail-spike cell to die upon subsequent CED-3 caspase expression. Like DRE-1, BLMP-1 was previously shown to promote developmental timing decisions in larva, and we find that both proteins function in parallel to inhibit tail-spike cell death. Importantly, homologs of both proteins also function together in mammalian B lymphocyte development, and control tumorigenesis in this cell type, in part by regulating apoptosis (Duan et al., 2012; Lin et al., 2007). Our results uncover a conserved genetic module regulating gene expression timing, which drives a cellular decision to live or die.

RESULTS

blmp-1 is required for tail-spike cell death

To identify genes regulating tail-spike cell death, we mutagenized animals carrying a tail-spike cell reporter, *aff-1* promoter::myristoylated-GFP (Ghose et al., 2018), and screened 21,000 F2 progeny for inappropriate tail-spike cell persistence in L1 larvae. Two such mutants, with allele designations *ns823* and *ns830*, were identified (Figure 1B and C). Whole

genome sequencing revealed that both carry lesions in the gene *blmp-1*, encoding a Zn-finger transcription factor homologous to mammalian BLIMP-1. *ns823* mutants harbor a splice-donor mutation in intron 6, and *ns830* animals contain two point mutations in exon 3, resulting in predicted A205V and K348Stop protein alterations. To confirm that *blmp-1* mutations are indeed causal for tail-spike cell survival, we examined animals carrying the previously-identified *blmp-1* alleles *tm548* and *s71*, and found that they also possess surviving tail-spike cells (Figure 1C). Likewise, RNAi against *blmp-1* perturbs tail-spike cell death (Table 1). Survival is independent of the reporter transgene we used, as *blmp-1* mutants carrying a *C. briggsae ced-3* promoter::GFP reporter transgene (Materials and Methods) also exhibit tail-spike cell persistence (Table 1). A fosmid clone spanning the *blmp-1* locus restores tail-spike cell death to *blmp-1* mutants (Figure 1C), as does expression of a *blmp-1* promoter::*blmp-1* cDNA::GFP transgene (Table 1). Importantly, expression of *blmp-1* cDNA specifically in the tail-spike cell can restore tail-spike cell death to the same extent as the fosmid (Figure 1D). Taken together, these studies suggest that *blmp-1* is required cell-autonomously for tail-spike cell death. Overexpression of *blmp-1* cDNA in the phasmid sheath cells, located in the tail region near the tail-spike cell, does not cause phasmid sheath cell death (Figure 1E). Thus, *blmp-1* is unlikely to be a direct component of the tail-spike cell killing apparatus, and is more likely to function as a regulator.

BLMP-1::GFP is detected in the tail-spike shortly after the cell is generated

Tail-spike cell death is initiated at the 3.2-fold stage of embryogenesis, ~550 minutes post-fertilization (Ghose et al., 2018; Sulston et al., 1983). To determine when *blmp-1* is expressed relative to cell death onset, we generated animals carrying a single copy *blmp-1* promoter::GFP transgene using PhiC31 integrase-mediated insertion (Yang et al., 2020), and crossed these with animals expressing the *aff-1* promoter::myristoyl-KatePH (mKatePH) tail-spike cell reporter. We found that *blmp-1* transcription is detected in the tail-spike cell as

early as the mKatePH reporter (1.5-fold stage; Figure 2A). *blmp-1* transcription continues until the tail-spike cell dies with a characteristic rounded refractile morphology at the 3.7-fold stage (Figure 2B-D).

To determine whether BLMP-1 protein accumulation follows its transcriptional expression pattern, we examined animals carrying the *cshIs41[BLMP-1::GFP]* single-copy translational reporter, in which GFP is fused to the BLMP-1 C terminus (Stec et al., 2021). We found that, like the transcriptional reporter, endogenous BLMP-1::GFP is detected in the tail-spike cell from the 1.5-fold stage until the cell dies (Figure 2E-H).

BLMP-1 represses *ced-9* transcription in the tail-spike cell

blmp-1 and its homologs have been shown to act as transcriptional repressors (Agawa et al., 2007; Nutt et al., 2007; Turner et al., 1994), raising the possibility that *blmp-1* promotes tail-spike cell death by inhibiting expression of a cell-protective gene. In *C. elegans*, CED-9/BCL-2 inhibits the apoptotic cascade. We therefore tested whether tail-spike cell survival in *blmp-1* mutants requires *ced-9*. These studies were performed in animals also homozygous for the weak *ced-3(n2427)* allele, which blocks *ced-9*-induced embryonic lethality without affecting tail-spike cell death (Chiorazzi et al., 2013; Maurer et al., 2007). We found that while *blmp-1(s71)*; *ced-3(n2427)* animals often possess surviving tail-spike cells, animals also homozygous for the *ced-9(n2812)* loss-of-function mutation do not (Figure 3A). A similar result was obtained using *blmp-1*(RNAi) (Figure 3B). Thus, *blmp-1* acts upstream of *ced-9* to promote tail-spike cell death, possibly by repressing *ced-9* gene expression.

To further examine this idea, we sought to examine the effect of *blmp-1* loss on *ced-9* transcription. Using a single-copy *ced-9* promoter::GFP transgene, we found that *ced-9* transcription is not detectable at the 1.5- and 2-fold stages and is barely observable at the 3.2-fold stage (Figure 4A-D). Notably, by examining GFP intensity under the same exposure

condition, we found that the *blmp-1(s71)* mutation weakly but significantly enhances *ced-9* transcription at the 3.2-fold stage (Figure 4E-H and P), showing that *blmp-1* represses *ced-9* transcription near the onset time of the tail-spike cell death. Intriguingly, *ced-9* transcription also appears to be upregulated in the *blmp-1(s71)* mutant in cells adjacent to the tail-spike cell at the 3.2- and 3.7-fold stages, suggesting that *blmp-1* may also regulate *ced-9* expression in these cells (Figure 2G and H).

BLMP-1 binds *ced-9* DNA regulatory sequences required for *ced-9* transcription

A search for Zn-finger transcription factor binding sites, within a 2 kb region upstream of the *ced-9* translation start site (http://zf.princeton.edu/), uncovered a 17 bp sequence within which is embedded the sequence TTTCAATTT, nearly identical to the previously-defined BLMP-1 consensus binding site TTTCACTTT (Gerstein et al., 2010) (Figure 5). To determine whether the Zn-finger domains of BLMP-1 can bind this sequence, we performed gel mobility shift assays. As shown in Figure 5, bacterially-produced maltose-binding protein (MBP) is unable to shift a 39-bp DNA fragment containing the putative binding site. However, a dose-dependent slower migrating band, indicative of protein-DNA binding, is observed when bacterially-expressed MBP::BLMP-1(ZnF) fusion protein, containing only the BLMP-1 Zn-finger domains, is used (Figure 5). This band is not evident when DNA of different sequence is used (mutant probe, changing TTTCAATTT to AGGGTTAGG). Importantly, a *ced-9* promoter::GFP reporter transgene harboring the mutant sequence ($P_{ced\text{-}9m}$*::*GFP) is no longer down-regulated and shows a similar expression level when compared to $P_{ced\text{-}9}$*::*GFP in the *blmp-1(s71)* mutant (Figure 4I-L and P). Moreover, the *blmp-1(s71)* mutation did not further enhance the expression of $P_{ced\text{-}9m}$*::*GFP (Figure 4 M and P). These results suggest that in the tail-spike cell, BLMP-1 directly binds the TTTCAATTT sequence upstream of the *ced-9* ATG, blocking *ced-9* gene expression.

BLMP-1 binding to *ced-9* regulatory sequences is required for tail-spike cell death

To assess the physiological significance of BLMP-1 DNA binding, we generated three sets of *ced-9(n2812); ced-3(n2427)* transgenic animals, carrying either a functional *ced-9* promoter::*ced-9*::GFP transgene, a *ced-9*Δ promoter::*ced-9*::GFP transgene lacking the BLMP-1 binding site TTTCAATTT, or a *ced-9m* transgene in which the *ced-9* promoter contains a mutant BLMP-1 binding site (changing TTTCAATTT to AGGGTTAGG). We found that while the wild-type transgene alone does not perturb tail-spike cell death, treatment of transgenic animals with *blmp-1* RNAi promotes tail-spike cell survival (Figure 3B). By contrast, the binding-site-deleted or binding-sequence-altered transgenes cause tail-spike cell survival, even without *blmp-1* RNAi. Survival is similar in extent to that observed in animals carrying the wild-type transgene and treated with *blmp-1* RNAi (Figure 3B). Moreover, *blmp-1* RNAi does not further enhance this survival (Figure 3B). These data reveal that BLMP-1 binding to *ced-9* regulatory DNA directly promotes tail-spike cell death.

***blmp-1* and *dre-1* independently down-regulate CED-9 to promote tail-spike cell death**

Mutations in the gene *dre-1*, encoding an F-box-type E3 ubiquitin ligase substrate-recognition component, block tail-spike cell death. DRE-1 has been shown to directly bind BLMP-1 and to mediate BLMP-1 degradation during larval development (Horn et al., 2014; Huang et al., 2014), suggesting opposite functions for DRE-1 and BLMP-1. However, we suspected that this may not be the case for the tail-spike cell, as *blmp-1* and *dre-1* mutants both harbor surviving tail-spike cells. We previously showed that *dre-1* acts upstream of *ced-9*, and that DRE-1 may target CED-9 protein for degradation (Chiorazzi et al., 2013). We therefore wondered whether the combined action of DRE-1 and BLMP-1 leads to synergistic reduction in CED-9 activity, ensuring tail-spike cell death fidelity. To test this, we examined mutants containing genetic lesions in either *blmp-1*, *dre-1*, or both. We found that tail-spike cell survival in animals carrying the *blmp-1(s71)* allele, encoding a protein

lacking Zn-finger DNA binding residues, could be enhanced by even weak mutations in *dre-1* (Figure 6A). Since BLMP-1 DNA binding is predicted to be abolished in *blmp-1(s71)* mutants (Huang et al., 2014), DRE-1 activity must therefore be independent of BLMP-1. Supporting this conclusion, RNAi against *dre-1* does not affect BLMP-1::GFP levels (Figure 2I-M). Conversely, *blmp-1* RNAi does not affect expression of the single-copy *dre-1* promoter::GFP transgene (Figure 6B-J). Furthermore, knockdown of *dre-1* does not increase *ced-9* transcription in the wild-type or *blmp-1(s71)* mutant (Figure 4N, O and P). Therefore, the combined action of BLMP-1 and DRE-1 is important to ensure loss of CED-9 activity, and cell death activation.

As previously reported, *ced-3* transcription initiates at the 3.2-fold stage when the tail-spike cell is about to die (Maurer et al., 2007). We confirmed this result using a single-copy transgene (Supplementary Figure S1), and examined the effect of *blmp-1* RNAi on this reporter. We found that *blmp-1* is not required for *ced-3* transcriptional activation (Supplementary Figure S1). BLMP-1 also functions with the genes *lin-29* and *daf-12* during gonadogenesis and larval development (Horn et al., 2014; Huang et al., 2014). Loss of *lin-29* or *daf-12*, however, does not affect tail-spike cell death (Table 1). Thus, our studies reveal a novel combinatorial action of BLMP-1 and DRE-1.

DISCUSSION

In this study, we identify an essential role for the BLMP-1/Blimp1 transcriptional repressor in tail-spike cell death. Our findings, together with previous studies, suggest dynamic and multi-layered control of tail-spike survival. At the 1.5-fold stage, low levels of *ced-9* fail to promote tail-spike cell death, as *ced-3* caspase expression is turned off. At the 3.2-fold stage of embryogenesis, when tail formation is complete, *ced-9* transcription is activated in the tail-spike cell and its adjacent cells, likely by a region-specific transcription factor. Three regulatory events counter this modest CED-9 accumulation and dismantle the pro-survival

state in the tail-spike cell: *ced-9* transcription is repressed by BLMP-1; CED-9 protein is degraded by DRE-1 E3 ubiquitin ligase; and *ced-3* caspase gene expression is induced by PAL-1, a caudal-like transcription factor (Maurer et al., 2007). Furthermore, mutations in the CED-9 regulator EGL-1/BH3-only weakly perturb tail-spike cell death, indicating that EGL-1-CED-9 binding also drives cell death. The combined effect of these events ensures activation of a tail-spike cell dismantling program at high fidelity. Cell elimination then proceeds through CED-3 caspase-dependent compartmentalized cell elimination (CCE) (Ghose et al., 2018).

We show here that *blmp-1* transcription and protein accumulation are detected in the tail-spike cell at the 1.5-fold stage, shortly after the cell is born. Like BLMP-1, PAL-1 is expressed prior to the onset of tail-spike cell death (Edgar et al., 2001). It is interesting that their respective target genes, the pro-survival gene *ced-9* and pro-apoptotic gene *ced-3*, and the other CED-9 regulator, DRE-1, are transcriptionally upregulated specifically at the 3.2-fold stage, indicating that other factors are involved in the time-specific upregulation of *ced-9*, *ced-3* and *dre-1*. It is unclear whether a common factor controls the expression of these three genes. It is possible that the cue initiating tail-spike death may emanate from neighboring hypodermal cells that signal completion of tail development. Uncovering the transcription factor/s that induce *ced-9*, *ced-3*, or *dre-1* expression may provide clues to signal identity.

Blimp-family members have been shown to control the timing of developmental processes in *C. elegans* (Horn et al., 2014; Huang et al., 2014), *Drosophila* (Agawa et al., 2007; Ng et al., 2006), zebrafish (Lee and Roy, 2006) and mice (Harper et al., 2011). In *C. elegans*, BLMP-1 and DRE-1 control the timing of several developmental events, including larval distal-tip cell migration and seam cell development (Horn et al., 2014; Huang et al., 2014). However, other timing genes, including *lin-29* and *daf-12*, are not required for tail-spike cell death (Table 1), suggesting that if BLMP-1 and DRE-1 function as a timing

regulator in the tail-spike cell the mechanism may be different. Consistent with this notion, it has been shown that DRE-1 mediates BLMP-1 proteolysis to temporally control distal tip cell migration and seam cell development (Horn et al., 2014; Huang et al., 2014), whereas DRE-1 does not appear to affect BLMP-1 protein levels in tail-spike cell death (Figure 2I-M).

FBXO11, the human homolog of DRE-1, has been reported to recognize and promote ubiquitin-mediated degradation of multiple Snail family members of zinc-finger transcription factors in mammalian cells (Jin et al., 2015). Interestingly, *C. elegans* Snail-like gene *ces-1*, which represses *egl-1* transcription in the NSM sister cells and therefore prevent their death, genetically interacts with *dre-1* in seam cell development (Jin et al., 2015; Metzstein and Horvitz, 1999; Thellmann et al., 2003). Loss of *ces-1* suppresses the precocious phenotype of seam cell development in the *dre-1* mutant, raising a possibility that CES-1 might function as a DRE-1 target during seam cell development. However, it is yet unclear whether CES-1 may be involved in regulation of tail-spike cell death, and if so, whether CES-1 might function as a DRE-1 target in the timing control of tail-spike cell death. Intriguingly, CED-3 plays a non-canonical role in regulating developmental timing in seam cell development by acting together with the Arg/N-end rule pathway (Weaver et al., 2017; Weaver et al., 2014). Specifically, CED-3 forms a complex with Arg/N-end rule E3 ligase UBR-1 and Arginyltransferase ATE-1 to efficiently cleave LIN-28, which is subsequently degraded through the Arg/N-end rule pathway, and prevent abnormal temporal seam cell divisions (Weaver et al., 2017). Therefore, several components involved in larval timing control appear to also function in tail-spike cell death.

Our studies also suggest that the model of cell death control we present here may be conserved. Indeed, Blimp-1 can drive apoptosis in mammals (Messika et al., 1998; Setz et al., 2018), and in immature WEHI 231 murine B-cell lymphoma cells this is accomplished through inhibition of the *bcl-2* family member A1 (Knodel et al., 1999). Furthermore, DRE-1 in the tail-spike cell, and its human homolog FBXO10, in B-cell lymphomas, interact with

CED-9 and BCL-2, respectively to promote apoptosis. Thus, our results demonstrate the power of using a simple, genetically facile model organism, *C. elegans*, for gene pathway discoveries in mammals.

MATERIALS AND METHODS

Strains

Animals were maintained at 20°C as described previously (Brenner, 1974). The Bristol N2 strain was used as wild type. The following alleles were used:

LGI: *blmp-1(ns823)*, *blmp-1(ns830)*, *blmp-1(s71)*, *blmp-1(tk41)*, *blmp-1(tm548)*, *blmp-1(tp5 and cshIs41[BLMP-1::GFP]*

LGIII: *ced-9(n2812)*.

LGIV: *ced-3(n2427)*.

LGV: *dre-1(dh99)*, *dre-1(dh279)*, and *dre-1(ns39)*.

LGX: *daf-12(rh61rh411)*.

Transgenic animals

Germ-line transformation was performed as described previously (Mello and Fire, 1995). To observe the tail-spike cell by GFP fluorescence, $P_{cbr\text{-}ced\text{-}3(0.8kb)}$*::gfp* (20 ng/µl) (pYW1233) was injected into wild-type animals with the co-injection marker $P_{myo\text{-}2}$*::gfp* (1 ng/µl) to generate *tpEx199*. The *tpEx199* extrachromosomal transgene was integrated into the genome by UV irradiation (Mariol et al., 2013) to generate *tpIs6*. *nsIs435* and *nsIs685* were also used to visualize tail-spike cell (Ghose et al., 2018). Single copy insertion of *gfp* reporters into LGII was performed based on the phiC31 recombination with kind help from John Wang and Shih-Peng Chan. All transgenic animals used in this work are listed in Supplementary Table S1.

Scoring tail-spike cell death

Tail-spike cell death in *tpIs6*, *nsIs431*, or *nsIs435* was scored at the L1 stage. Animals were synchronized by treating gravid hermaphrodites with alkaline bleach and allowing the eggs to hatch in M9 medium overnight. Synchronized L1s were then mounted on slides on 2% agarose-water pads, anaesthetized in 10 mM sodium azide and examined on a Zeiss Axio-Scope A1 under Nomarski optics and wide-field fluorescence using a 40x or 100X lens. The tail-spike cell was identified by reporter fluorescence as well as by its location and morphology.

Mutagenesis and mutant identification

nsIs435 animals were mutagenized using 75 mM ethylmethanesulfonate (M0880, Sigma) for 4 h at 20°C. Approximately 21,000 F2 progeny were screened for tail-spike cell persistence on a Zeiss Axio-Scope A1 using a 40x lens. *blmp-1* was identified as the causal gene using whole genome sequencing, fosmid rescue of *ns830* and *ns823*, and candidate gene analysis.

RNA interference

RNAi was performed by microinjecting double-stranded RNA as described previously (Fire et al., 1998). The *blmp-1* RNAi construct was obtained from the Ahringer RNAi library (Kamath et al., 2003). The *dre-1* and *lin-29* RNAi constructs were made by insertion of the corresponding cDNA fragments into the L4440 vector (Huang et al., 2014). *blmp-1* and *dre-1* RNAi resulted in gene knockdown, as >80% of animals exhibited a dumpy body shape or larval arrest, respectively. *lin-29* RNAi knockdown was confirmed as >80% of animals contained a distal tip cell migration defect in the *dre-1(dh99)* mutant (Huang et al., 2014).

Fluorescence images and quantification

All images were captured using a Zeiss AxioImager M2 microscope (Zeiss) equipped with a charge-coupled device camera with an exposure time of 500 ms for GFP and 500 ms for mKatePH. The GFP signals within the tail-spike cells (I_{GFP}) and their neighboring regions outside the embryos(B_{GFP}) were quantified using Image J and GFP intensities were scaled as I_{GFP}-B_{GFP}. Representative images of different stages are from different embryos. Images were deconvolved to remove out-of-focus light.

Molecular biology

The tail-spike-cell-specific rescue construct (pPG267) was generated by Gibson cloning (Gibson et al., 2009). *blmp-1* cDNA was amplified from synthesized *blmp-1* in the pUC57 vector (Gene Universal) using the primers ggaacgcatgcctgcaggtcgactctagaggatccccgggaaaatgggtcaaggaagtggggatg and taatggtagcgaccggcgctcagttggaattctacgaatgttatggataatgcggcaatccgagg. pPG161 (containing the *aff-1* promoter) was used as the backbone. To generate $P_{cbr\text{-}ced\text{-}3(0.8kb)}$*::gfp,* 800 bp upstream of the *ced-3* start codon were amplified from *C. briggsae* genomic DNA by PCR using primers 5'-TGAACGATTTCCCTCATAAGCAC-3' and 5'-CCTCCTCACCGAATGCTAGTCTG-3'. The resulting PCR fragment was cloned into the SmaI site of pPD95.75 to generate pYW1233. The transcriptional reporters of *blmp-1* were described previously (Huang et al., 2014). The transcriptional reporter of *dre-1* was constructed by amplifying the 4 kb upstream of *dre-1* start codon from *C. elegans* by PCR using primers 5'-GGATCCCGAGGGGACATCGAGATAG-3' and 5'-GGATCCTTCCTGGCCAACCAGAGAC-3' and the resulting PCR fragment was cloned into the BamHI site of pPD95.75. These reporters were then inserted into a modified phiC31 vector (P5-5_pCG150_phiC31_V2), a gift from Shih-Peng Chan at National Taiwan University) by SbfI and ApaI. The transcriptional and translational reporters of *ced-9* were

constructed using MultiSite Gateway® Three-Fragment Vector Construction Kit (Invitrogen) using following primers:

5’-GGGGACAACTTTGTATAGAAAAGTTGGTGGGCCTGATGGTACCAATTAG-3’

and

5’-GGGGACTGCTTTTTTGTACAAACTTGCTAAAATTTTTATTCGTTTTCATAATCA TAATATAC-3’ for *ced-9* promoter and 5’

-GGGGACAAGTTTGTACAAAAAAGCAGGCTGATGACACGCTGCACGGCGG-3’ and

5’-GGGGACCACTTTGTACAAGAAAGCTGGGTTCTTCAAGCTGAACATCATCCGCC -3’ for *ced-9* cDNA. The deletion or mutation of BLMP-1 binding site TTTCAATTT (922-930 bp upstream of the ATG of *ced-9*) was constructed by site-directed mutagenesis. Briefly, the plasmid $P_{ced\text{-}9}$*::gfp* and $P_{ced\text{-}9}$*::ced-9::gfp* mentioned above were amplified by primers, 5’-ACGCACCGCCCTGTTTCTTTTGATAAGAAAATCAGCATTG-3’ and

5’-CAATGCTGATTTTCTTATCAAAAGAAACAGGGCGGTGCGT-3’ for deleted BLMP-1 binding site and

5’-ACGCACCGCCCTGTTTCTTTAGGGTTAGGTGATAAGAAAATCAGCATTG-3’ and

5’-CAATGCTGATTTTCTTATCACCTAACCCTAAAGAAACAGGGCGGTGCGT-3’ for mutated BLMP-1 binding site, and the resulting PCR products were treated with *Dpn*I and then transformed to competent cells. Plasmids were verified by sequencing.

Electrophoretic mobility shift assay (EMSA)

Expression of MBP and MBP::BLMP-1(ZnF) were induced in the *Escherichia coli* strain BL21 by isopropyl thiogalactoside (IPTG), followed by the purification using amylase resin (NEB) and elution buffer (10 mM maltose, 20 mM Tris-HCl, 200 mM NaCl, 1 mM EDTA, 1 mM azide, and 10 mM Dithiothreitol). EMSA was performed using LightShift Chemiluminescent EMSA kits (Pierce) according to the manufacturer’s instruction. Briefly, purified protein was incubated with biotin-labeled probe with 10X binding buffer plus 250

μM $ZnCl_2$ at room temperature for 20 minutes, and the mixture was separated on a 5% non-denaturing polyacrylamide gel in 0.5X TBE. The DNA was then transferred to a charged nylon membrane (Millipore), cross-linked with UV light using the auto crosslink option on a UV Stratalinker 1800 (Stratagene), and detected following the manufacturer's protocol.

Statistical analysis

Student's two-tailed unpaired *t*-test was used and data were considered to be significantly different when $P<0.05$.

Conflict of Interest

The authors declare no conflict of interest.

ACKNOWLEDGEMENTS

We thank A. Fire for the *gfp* vectors, the *Caenorhabditis* Genetics Center, supported by a grant from the National Institutes of Health, for providing strains, and the Technology Commons in the College of Life Science and Center for Systems Biology at NTU, and the *C. elegans* core facility (supported by a grant from the National Core Facility for Biopharmaceuticals, the National Ministry of Science and Technology (MOST) in Taiwan) for technical and material support. We thank John Wang and Shih-Peng Chan for providing the technical and material support of the phiC31 recombination system. The strain *cshIs41[BLMP-1::GFP]* is a kind gift from Dr. Christopher M Hammell. This work was supported in part by MOST and NTU (NTU-107L880302) grants to YCW, NIH grant F32HD089640 to P.G., and NIH grant R35NS105094 to S.S.

Author contributions

HSJ, PG, HFH, JCW, SS, and YCW conceived and designed experiments, and wrote the manuscript. HSJ, PG, HFH, YZW, YYT, HCL, WCT, and JCW performed the experiments and analyzed the data.

REFERENCES

Abraham, M. C., Lu, Y. and Shaham, S. (2007). A morphologically conserved nonapoptotic program promotes linker cell death in Caenorhabditis elegans. *Developmental cell* **12**, 73-86.

Agawa, Y., Sarhan, M., Kageyama, Y., Akagi, K., Takai, M., Hashiyama, K., Wada, T., Handa, H., Iwamatsu, A., Hirose, S., et al. (2007). Drosophila Blimp-1 is a transient transcriptional repressor that controls timing of the ecdysone-induced developmental pathway. *Molecular and cellular biology* **27**, 8739-8747.

Brenner, S. (1974). The genetics of Caenorhabditis elegans. *Genetics* **77**, 71-94.

Chen, F., Hersh, B. M., Conradt, B., Zhou, Z., Riemer, D., Gruenbaum, Y. and Horvitz, H. R. (2000). Translocation of C. elegans CED-4 to nuclear membranes during programmed cell death. *Science* **287**, 1485-1489.

Chiorazzi, M., Rui, L., Yang, Y., Ceribelli, M., Tishbi, N., Maurer, C. W., Ranuncolo, S. M., Zhao, H., Xu, W., Chan, W. C., et al. (2013). Related F-box proteins control cell death in Caenorhabditis elegans and human lymphoma. *Proceedings of the National Academy of Sciences of the United States of America* **110**, 3943-3948.

Conradt, B. and Horvitz, H. R. (1998). The C. elegans protein EGL-1 is required for programmed cell death and interacts with the Bcl-2-like protein CED-9. *Cell* **93**, 519-529.

Conradt, B., Wu, Y. C. and Xue, D. (2016). Programmed Cell Death During Caenorhabditis elegans Development. *Genetics* **203**, 1533-1562.

del Peso, L., Gonzalez, V. M., Inohara, N., Ellis, R. E. and Nunez, G. (2000). Disruption of the CED-9.CED-4 complex by EGL-1 is a critical step for programmed cell death in Caenorhabditis elegans. *The Journal of biological chemistry* **275**, 27205-27211.

del Peso, L., Gonzalez, V. M. and Nunez, G. (1998). Caenorhabditis elegans EGL-1 disrupts the interaction of CED-9 with CED-4 and promotes CED-3 activation. *The Journal of biological chemistry* **273**, 33495-33500.

Duan, S., Cermak, L., Pagan, J. K., Rossi, M., Martinengo, C., di Celle, P. F., Chapuy, B., Shipp, M., Chiarle, R. and Pagano, M. (2012). FBXO11 targets BCL6 for degradation and is inactivated in diffuse large B-cell lymphomas. *Nature* **481**, 90-93.

Edgar, L. G., Carr, S., Wang, H. and Wood, W. B. (2001). Zygotic expression of the caudal homolog pal-1 is required for posterior patterning in Caenorhabditis elegans embryogenesis. *Dev Biol* **229**, 71-88.

Fielenbach, N., Guardavaccaro, D., Neubert, K., Chan, T., Li, D., Feng, Q., Hutter, H., Pagano, M. and Antebi, A. (2007). DRE-1: an evolutionarily conserved F box protein that regulates C. elegans developmental age. *Developmental cell* **12**, 443-455.

Fire, A., Xu, S., Montgomery, M. K., Kostas, S. A., Driver, S. E. and Mello, C. C. (1998). Potent and specific genetic interference by double-stranded RNA in Caenorhabditis elegans. *Nature* **391**, 806-811.

Fuchs, Y. and Steller, H. (2011). Programmed cell death in animal development and disease. *Cell* **147**, 742-758.

Gerstein, M. B., Lu, Z. J., Van Nostrand, E. L., Cheng, C., Arshinoff, B. I., Liu, T., Yip, K. Y., Robilotto, R., Rechtsteiner, A., Ikegami, K., et al. (2010). Integrative analysis of the Caenorhabditis elegans genome by the modENCODE project. *Science* **330**, 1775-1787.

Ghose, P., Rashid, A., Insley, P., Trivedi, M., Shah, P., Singhal, A., Lu, Y., Bao, Z. and Shaham, S. (2018). EFF-1 fusogen promotes phagosome sealing during cell process clearance in Caenorhabditis elegans. *Nat Cell Biol* **20**, 393-399.

Gibson, D. G., Young, L., Chuang, R. Y., Venter, J. C., Hutchison, C. A., 3rd and Smith, H. O. (2009). Enzymatic assembly of DNA molecules up to several hundred kilobases. *Nature methods* **6**, 343-345.

Harper, J., Mould, A., Andrews, R. M., Bikoff, E. K. and Robertson, E. J. (2011). The transcriptional repressor Blimp1/Prdm1 regulates postnatal reprogramming of intestinal enterocytes. *Proceedings of the National Academy of Sciences of the United States of America* **108**, 10585-10590.

Hengartner, M. O. and Horvitz, H. R. (1994). C. elegans cell survival gene ced-9 encodes a functional homolog of the mammalian proto-oncogene bcl-2. *Cell* **76**, 665-676.

Horn, M., Geisen, C., Cermak, L., Becker, B., Nakamura, S., Klein, C., Pagano, M. and Antebi, A. (2014). DRE-1/FBXO11-dependent degradation of BLMP-1/BLIMP-1 governs C. elegans developmental timing and maturation. *Developmental cell* **28**, 697-710.

Huang, S. (1994). Blimp-1 is the murine homolog of the human transcriptional repressor PRDI-BF1. *Cell* **78**, 9.

Huang, T. F., Cho, C. Y., Cheng, Y. T., Huang, J. W., Wu, Y. Z., Yeh, A. Y., Nishiwaki, K., Chang, S. C. and Wu, Y. C. (2014). BLMP-1/Blimp-1 regulates the spatiotemporal cell migration pattern in C. elegans. *PLoS genetics* **10**, e1004428.

Jin, Y., Shenoy, A. K., Doernberg, S., Chen, H., Luo, H., Shen, H., Lin, T., Tarrash, M., Cai, Q., Hu, X., et al. (2015). FBXO11 promotes ubiquitination of the Snail family of transcription factors in cancer progression and epidermal development. *Cancer letters* **362**, 70-82.

Kamath, R. S., Fraser, A. G., Dong, Y., Poulin, G., Durbin, R., Gotta, M., Kanapin, A., Le Bot, N., Moreno, S., Sohrmann, M., et al. (2003). Systematic functional analysis of the Caenorhabditis elegans genome using RNAi. *Nature* **421**, 231-237.

Keller, A. D. and Maniatis, T. (1991). Identification and characterization of a novel repressor of beta-interferon gene expression. *Genes & development* **5**, 868-879.

Knodel, M., Kuss, A. W., Lindemann, D., Berberich, I. and Schimpl, A. (1999). Reversal of Blimp-1-mediated apoptosis by A1, a member of the Bcl-2 family. *European journal of immunology* **29**, 2988-2998.

Kutscher, L. M. and Shaham, S. (2017). Non-apoptotic cell death in animal development. *Cell Death Differ* **24**, 1326-1336.

Lee, B. C. and Roy, S. (2006). Blimp-1 is an essential component of the genetic program controlling development of the pectoral limb bud. *Developmental biology* **300**, 623-634.

Lin, F. R., Kuo, H. K., Ying, H. Y., Yang, F. H. and Lin, K. I. (2007). Induction of apoptosis in plasma cells by B lymphocyte-induced maturation protein-1 knockdown. *Cancer research* **67**, 11914-11923.

Mariol, M. C., Walter, L., Bellemin, S. and Gieseler, K. (2013). A rapid protocol for integrating extrachromosomal arrays with high transmission rate into the C. elegans genome. *Journal of visualized experiments : JoVE*, e50773.

Maurer, C. W., Chiorazzi, M. and Shaham, S. (2007). Timing of the onset of a developmental cell death is controlled by transcriptional induction of the C. elegans ced-3 caspase-encoding gene. *Development* **134**, 1357-1368.

Mello, C. and Fire, A. (1995). DNA transformation. *Methods in cell biology* **48**, 451-482.

Messika, E. J., Lu, P. S., Sung, Y. J., Yao, T., Chi, J. T., Chien, Y. H. and Davis, M. M. (1998). Differential effect of B lymphocyte-induced maturation protein (Blimp-1) expression on cell fate during B cell development. *The Journal of experimental medicine* **188**, 515-525.

Metzstein, M. M. and Horvitz, H. R. (1999). The C. elegans cell death specification gene ces-1 encodes a snail family zinc finger protein. *Mol Cell* **4**, 309-319.

Nagata, S. (2018). Apoptosis and Clearance of Apoptotic Cells. *Annual review of immunology* **36**, 489-517.

Ng, T., Yu, F. and Roy, S. (2006). A homologue of the vertebrate SET domain and zinc finger protein Blimp-1 regulates terminal differentiation of the tracheal system in the Drosophila embryo. *Development genes and evolution* **216**, 243-252.

Nutt, S. L., Fairfax, K. A. and Kallies, A. (2007). BLIMP1 guides the fate of effector B and T cells. *Nature reviews. Immunology* **7**, 923-927.

Setz, C. S., Hug, E., Khadour, A., Abdelrasoul, H., Bilal, M., Hobeika, E. and Jumaa, H. (2018). PI3K-Mediated Blimp-1 Activation Controls B Cell Selection and Homeostasis. *Cell reports* **24**, 391-405.

Stec, N., Doerfel, K., Hills-Muckey, K., Ettorre, V. M., Ercan, S., Keil, W. and Hammell, C. M. (2021). An Epigenetic Priming Mechanism Mediated by Nutrient Sensing Regulates Transcriptional Output during C. elegans Development. *Current biology : CB* **31**, 809-826 e806.

Sulston, J. E. and Horvitz, H. R. (1977). Post-embryonic cell lineages of the nematode, Caenorhabditis elegans. *Developmental biology* **56**, 110-156.

Sulston, J. E., Schierenberg, E., White, J. G. and Thomson, J. N. (1983). The embryonic cell lineage of the nematode Caenorhabditis elegans. *Developmental biology* **100**, 64-119.

Suzanne, M. and Steller, H. (2013). Shaping organisms with apoptosis. *Cell death and differentiation* **20**, 669-675.

Thellmann, M., Hatzold, J. and Conradt, B. (2003). The Snail-like CES-1 protein of C. elegans can block the expression of the BH3-only cell-death activator gene egl-1 by antagonizing the function of bHLH proteins. *Development* **130**, 4057-4071.

Turner, C. A., Jr., Mack, D. H. and Davis, M. M. (1994). Blimp-1, a novel zinc finger-containing protein that can drive the maturation of B lymphocytes into immunoglobulin-secreting cells. *Cell* **77**, 297-306.

Weaver, B. P., Weaver, Y. M., Mitani, S. and Han, M. (2017). Coupled Caspase and N-End Rule Ligase Activities Allow Recognition and Degradation of Pluripotency Factor LIN-28 during Non-Apoptotic Development. *Dev Cell* **41**, 665-673 e666.

Weaver, B. P., Zabinsky, R., Weaver, Y. M., Lee, E. S., Xue, D. and Han, M. (2014). CED-3 caspase acts with miRNAs to regulate non-apoptotic gene expression dynamics for robust development in C. elegans. *eLife* **3**, e04265.

Yang, F. J., Chen C. N., Chang T., Cheng T. W., Chang N. C., Kao C. Y., Lee C. C., Huang Y. C., Chan S. P. and Wang J. phiC31 integrase for recombination mediated single copy insertion and genome manipulation in C. elegans. BioRxiv 2020.11.25.398784 [Preprint]. Available from: https://doi.org/10.1101/2020.11.25.398784.

Yang, X., Chang, H. Y. and Baltimore, D. (1998). Essential role of CED-4 oligomerization in CED-3 activation and apoptosis. *Science* **281**, 1355-1357.

Yuan, J., Shaham, S., Ledoux, S., Ellis, H. M. and Horvitz, H. R. (1993). The C. elegans cell death gene ced-3 encodes a protein similar to mammalian interleukin-1 beta-converting enzyme. *Cell* **75**, 641-652.

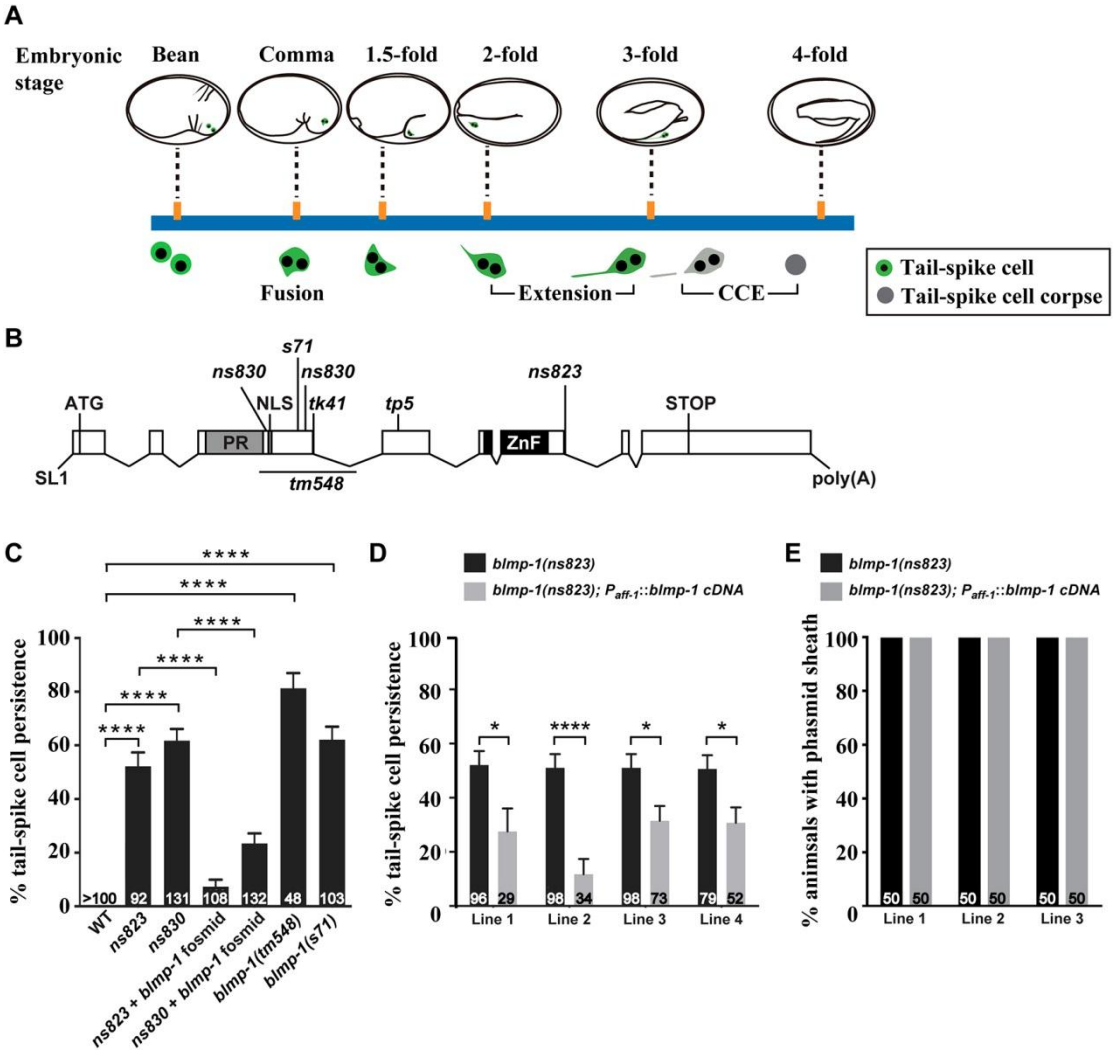

Figure 1. *blmp-1* is required for tail-spike cell death.

(A) A schematic diagram shows tail-spike cell development during embryogenesis. (B) Gene structure of *blmp-1*. The boxes indicate exons. The SL1 trans-spliced leader, initiation codon and stop codon are shown. The regions encoding the PRDI-BF1-RIZ1 homologous region (PR) domain, nuclear localization signal (NLS), and zinc finger motifs (ZnF) are indicated. The positions of the *blmp-1* mutant alleles, including the region corresponding to the *tm548* deletion, are marked. *s71*, *tk41*, and *tp5* have, respectively, non-sense mutations in codon 281, 381, or 434, and are predicted to encode truncated BLMP-1 proteins without zinc fingers. (C) *blmp-1* is necessary for tail-spike cell death. The tail-spike cell death defects of the indicated genotypes were scored. (D) *blmp-1* acts cell-autonomously to promote tail-spike cell death. The *blmp-1(ns823)* worms with or without expressing the transgenic *blmp-1* cDNA under the control of *aff-1* promoter was scored. Four independent transgenic lines were analyzed. (E) *blmp-1* does not induce cell death in phasmid sheath cells. Three independent transgenic lines were analyzed. (C, D and E) All animals carried the marker *nsIs435*, which is *aff-1*

promoter-driven myristoylated GFP and labels the tail-spike cell and phasmid sheath cells (Ghose et al., 2018), and were scored at the L1 stage for tail-spike cell or phasmid sheath cell survival. The number of worms analyzed is shown inside the bars. Data shown are mean ± s.e.m. * indicates $P<0.05$ and **** $P<0.0001$ in a two-tailed unpaired *t*-test.

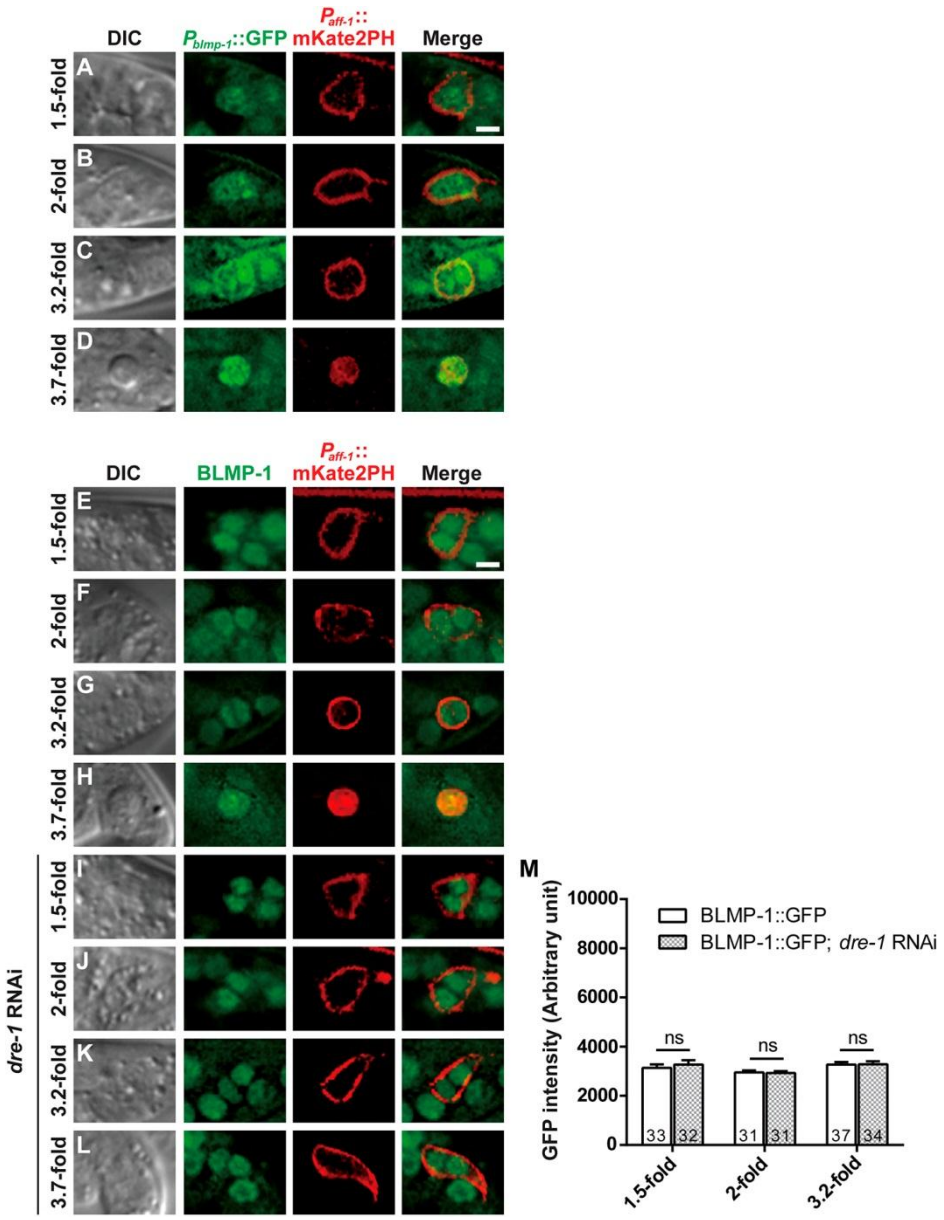

Figure 2. *blmp-1* is expressed in the tail-spike cell since the 1.5-fold embryonic stage. (A-L) Representative DIC, GFP, mKate, and merged images of wild-type (A-H) and *dre-1(RN*Ai) (I-L) embryos expressing *tpIs9[*P_{blmp-1}*::gfp]* (A-D) or *cshIs41[BLMP-1::GFP]* (E-L) at the indicated stage. The P_{aff-1}*::*mKatePH was used to mark the tail-spike cell. Scale bar, 2 μm. (M) The expression level of BLMP-1::GFP in the tail-spike cell of wild-type and *dre-1(RNAi)* embryos was measured as described in Materials and Methods. Data shown are mean ± s.e.m. The number of embryos analyzed is shown in the bar. ns indicates no statistical difference (P>0.05) in a two-tailed unpaired *t*-test.

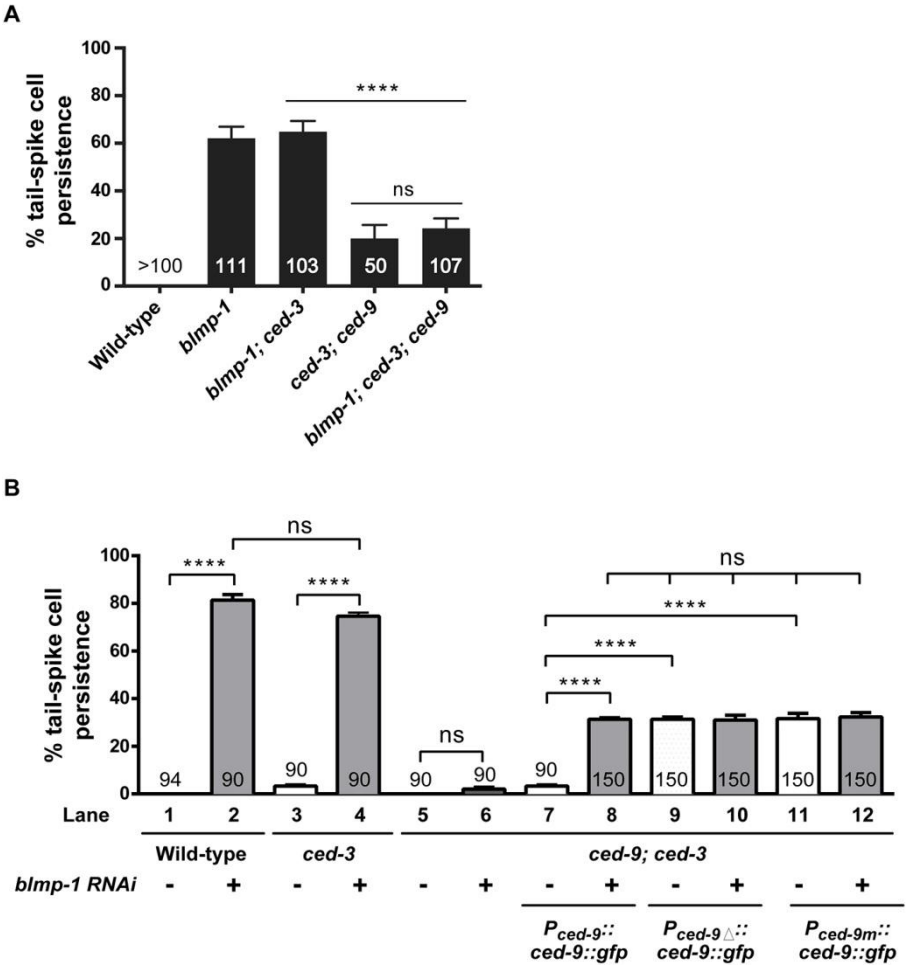

Figure 3. *blmp-1* genetically acts upstream of *ced-9* to promote tail-spike cell death. (A) Loss of *ced-9* suppresses the tail-spike cell death defect in the *blmp-1* mutant. The tail-spike cell death defects of the indicated genotypes were scored at the L1 stage. All animals contain the tail-spike cell marker *nsIs435* (Ghose et al., 2018). (B) Overexpression of *ced-9* results in tail-spike cell persistence in a *blmp-1*-dependent manner. The percentage of tail-spike cell persistence was scored in the L1 larvae of the *ced-3;ced-9* double mutants with or without the transgene ($P_{ced\text{-}9}$*::ced-9::gfp*, $P_{ced\text{-}9\Delta}$*::ced-9::gfp*, or $P_{ced\text{-}9m}$*::ced-9::gfp*) and with (+) or without (-) the *blmp-1* RNAi treatment. The number of worms analyzed is shown inside bars. Data shown are mean ± s.e.m. At least three biological replicates were analyzed for each genotype. **** indicates $P<0.0001$ and ns no statistical difference ($P>0.05$) in a two-tailed unpaired *t*-test. Alleles used were *blmp-1(s71)*, *ced-3(n2427)*, and *ced-9(n2812)*. The $P_{cbr\text{-}ced\text{-}3(0.8kb)}$*::gfp* (B, bars 1-6) or $P_{cbr\text{-}ced\text{-}3(0.8kb)}$*::mrfp* (B, bars 7-12) was used as a tail-spike cell marker.

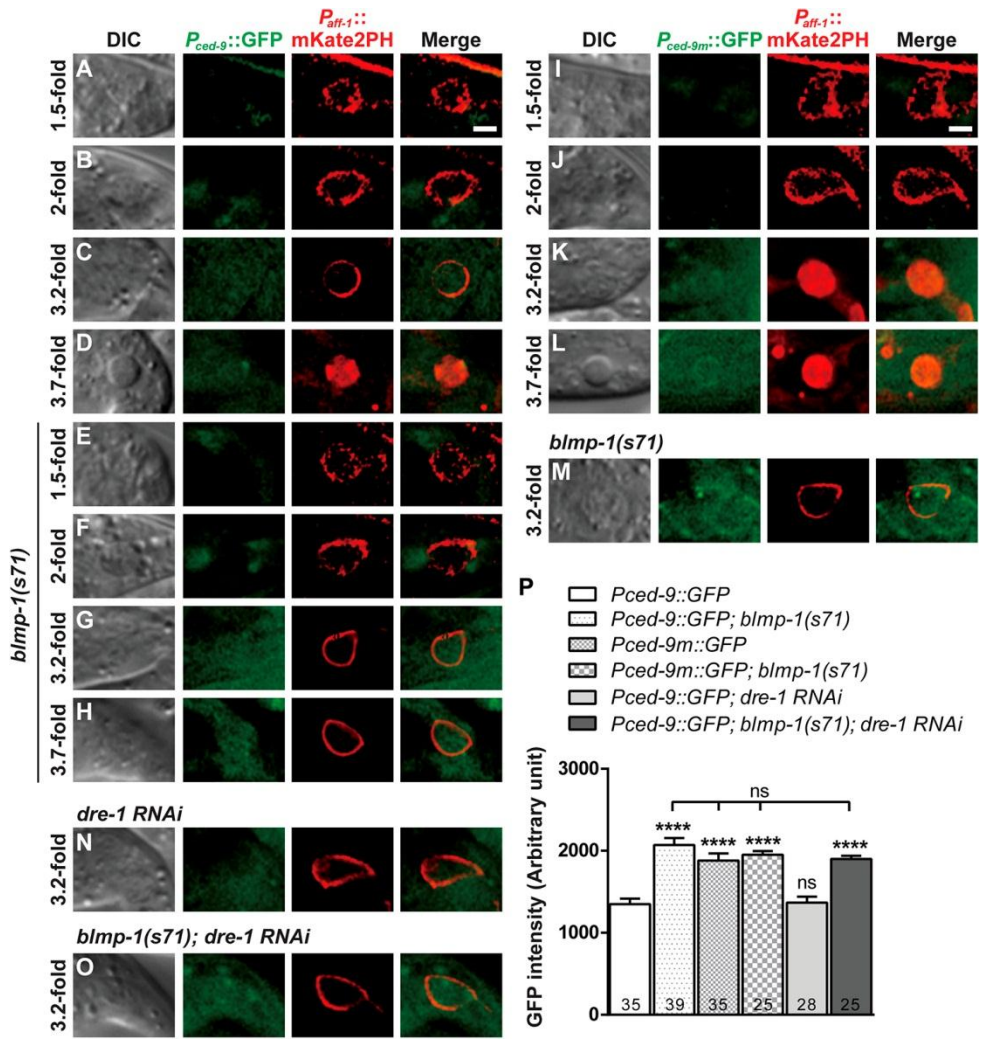

Figure 4. BLMP-1 represses *ced-9* transcription in the tail-spike cell at the 3.2-fold stage, shortly before the cell dies.

(A-O) Representative DIC, GFP, mKatePH, and merged images of wild-type (A-D), *blmp-1(s71)* (E-H), *dre-1 RNAi* (N) or *blmp-1(s71); dre-1(RNAi)* (O) embryos expressing *tpIs13[*$P_{ced\text{-}9}$*:: gfp]* or wild-type (I-L) or *blmp-1(s71)* (M) embryos expressing *tpIs15[*$P_{ced\text{-}9m}$*::gfp]* at the indicated stage. The $P_{aff\text{-}1}$*::*mKatePH was used to mark the tail-spike cell. Scale bar, 2 μm. (P) The expression level of wild-type, *blmp-1(s71), dre-1(RNAi)* or *blmp-1(s71); dre-1 (RNAi)* embryos expressing *tpIs13[*$P_{ced\text{-}9}$*:: gfp]*, or wild-type or *blmp-1(s71)* embryos expressing *tpIs15[*$P_{ced\text{-}9m}$*::gfp]* at the 3.2-fold stage was measured as described in Materials and Methods. Data shown are mean ± s.e.m. The number of embryos analyzed is shown in the bar. **** indicates $P<0.001$ in a two-tailed unpaired *t*-test. ns indicates no statistical difference ($P>0.05$).

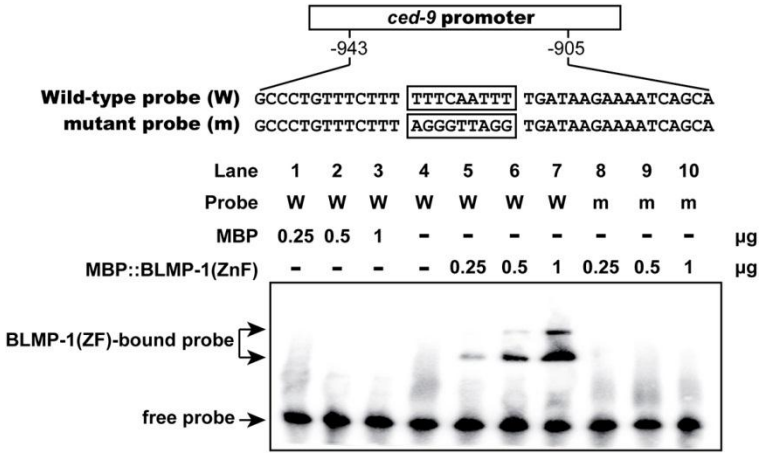

Figure 5. BLMP-1 directly binds to the *ced-9* promoter.

The Zn finger domain of BLMP-1 directly binds to the *ced-9* promoter in an EMSA assay. Different amounts of the indicated proteins (0.25, 0.5, or 1mg) were added to the wild-type *ced-9* probe (W), which contained the sequence from -943 to -905 upstream of the start codon of *ced-9*, or mutant *ced-9* probe (m), which changed the consensus BLMP-1 binding sequence from TTTCAATTT to AGGGTTAGG. The interaction between the indicated probe and protein was analyzed as described in Materials and Methods. The experiment was repeated three times.

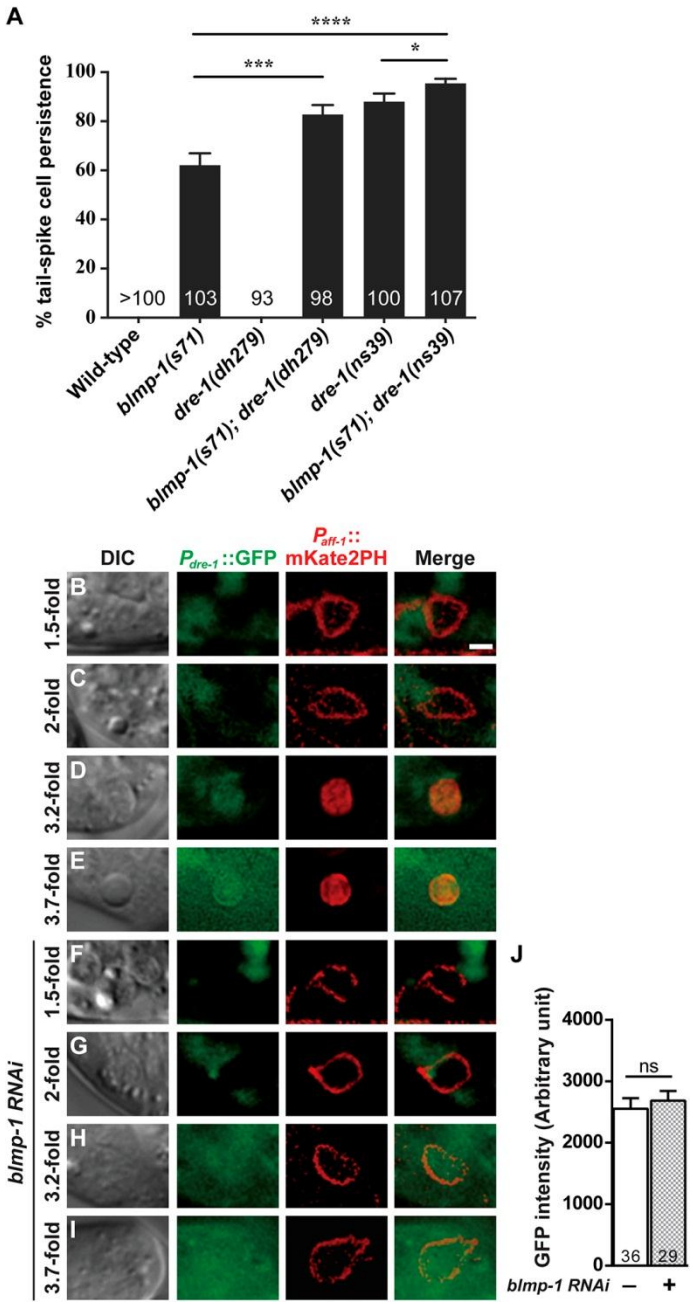

Figure 6. *blmp-1* and *dre-1* do not regulate each other during tail-spike cell death.

(A) The survival rate of tail-spike cell in the indicated genotypes. (B-I) Representative DIC, GFP, mKatePH, and merged images of embryos expressing *tpIs11[*$P_{dre\text{-}1}$*::gfp]* at the indicated stage. The $P_{aff\text{-}1}$::mKatePH was used to mark the tail-spike cell. Scale bar, 2 μm. (J) The expression level of $P_{dre\text{-}1}$*:: gfp* in the tail-spike cell at the 3.2-fold stage was measured as described in Materials and Methods. Data shown are mean ± s.e.m. The number of embryos analyzed is shown in the bar. ns indicates no statistical difference (P>0.05) in a two-tailed unpaired *t*-test.

Table 1 *blmp-1* and *dre-1*, but not *lin-29* and *daf-12*, are essential for tail-spike cell death.

Genotypes	% L1 larvae possessing the tail-spike cell (number of worms analyzed)
Wild-type	4 (50)
blmp-1(s71)	90 (50)
blmp-1(tk41)	65 (20)
blmp-1(tm548)	65 (20)
blmp-1(tp5)	80 (20)
blmp-1(RNAi)	85 (50)
blmp-1(s71); tpEx481[a]	51 (45)
dre-1(dh99)	20 (50)
dre-1(dh99); dre-1(RNAi)	82 (221)
lin-29(RNAi)	0 (50)
daf-12(rh61rh411)	0 (50)
daf-12(rh61rh411); lin-29(RNAi)	0 (50)

These strains contain the integrated transgene *tpIs6[*$P_{cbr\text{-}ced\text{-}3(0.8kb)}$*::gfp+*$P_{myo\text{-}2}$*::gfp]*. The RNAi experiment was performed by microinjecting double-stranded RNA of *blmp-1*, *dre-1*, or *lin-29* as indicated. [a]*tpEx481* contains $P_{blmp\text{-}1}$*::blmp-1::gfp,* $P_{cbr\text{-}ced\text{-}3}$*::mrfp,* and $P_{ttx\text{-}3}$*::gfp.*

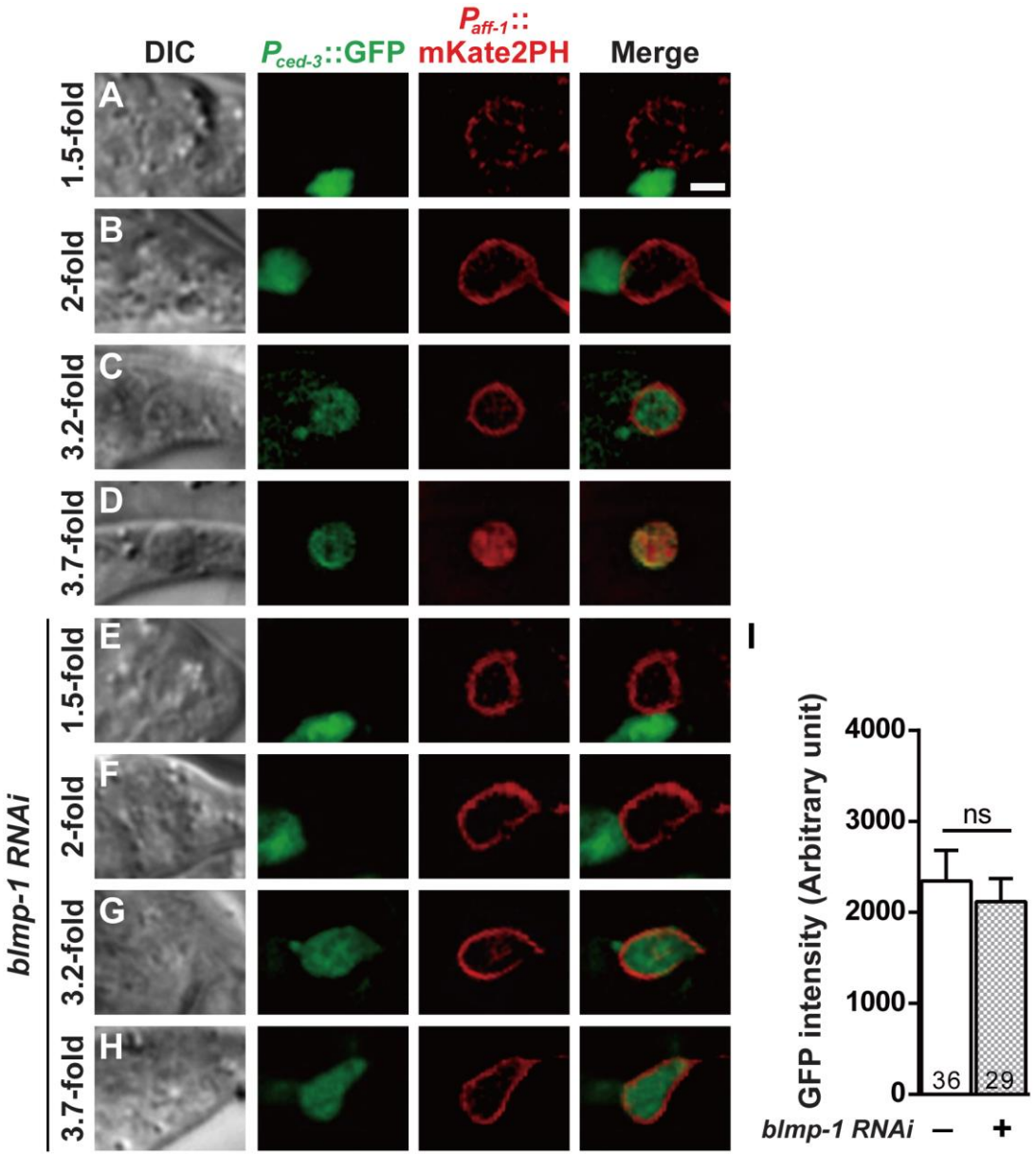

Fig. S1. The transcription of *ced-3* in the tail-spike cell is initiated at the 3.2-fold stage, shortly before the cell dies. (A-H) Representative DIC, GFP, mKate, and merged images of embryos expressing *tpIs16[*$P_{ced\text{-}3}$*::gfp]* at the indicated stage. The$P_{aff\text{-}1}$*::*mKatePH was used to mark the tail-spike cell. Scale bar, 2 μm. (I) The expression level of $P_{ced\text{-}3}$*:: gfp* in the tail-spike cell at the 3.2-fold stage was measured as described in Materials and Methods. Data shown are mean ± s.e.m. The number of embryos analyzed is shown in the bar. ns indicates no statistical difference (P>0.05) in a two-tailed unpaired *t*-test.

TableS1. Transgenes

Transgene	Injected plasmids and concentrations	Figures
nsIs435	*nsIs435[P_{aff-1}::myrGFP; coelomocyte::RFP]*	Figure 1, 3, and 6
nsEx6304	10 ng/μL *blmp-1* fosmid + 5 ng/μL *P_{cdh-3}::mCherry* + 0.5 ng/μL *P_{myo-2}::gfp*	Figure 1
nsEx6305	5 ng/μL *P_{aff-1}::blmp-1 cDNA* + 5 ng/μL *P_{cdh-3}::mCherry* + 0.5 ng/μL *P_{myo-2}::gfp*	Figure 1
tpIs6	*tpIs6[$P_{cbr-ced-3(0.8kb)}$::gfp; P_{myo-2}::gfp]*	Figure 3, and Table 1
nsIs685	*nsIs685[P_{aff-1}::mKate2PH; coelomocyte::RFP]*	Figure 2, 4, 6, and S1
tpIs9	*tpIs9[P_{blmp-1}::gfp]*	Figure 2
cshIs41	*cshIs41[BLMP-1::GFP]*	Figure 2
tpEx798	50 ng/μL *P_{ced-9}::ced-9::gfp* + 50 ng/μL *$P_{cbr-ced-3(0.8kb)}$::mrfp* + 50 ng/μL *P_{ttx-3}::gfp*	Figure 3
tpEx799		
tpEx800		
tpEx807	50 ng/μL *$P_{ced-9\Delta}$::ced-9::gfp* + 50 ng/μL *$P_{cbr-ced-3(0.8kb)}$::mrfp* + 50 ng/μL *P_{ttx-3}::gfp*	Figure 3
tpEx808		
tpEx809		
tpEx976	50 ng/μL *P_{ced-9m}::ced-9::gfp* + 50 ng/μL *$P_{cbr-ced-3(0.8kb)}$::mrfp* + 50 ng/μL *P_{ttx-3}::gfp*	Figure 3
tpEx977		
tpEx978		
tpIs13	*tpIs13[P_{ced-9}::gfp]*	Figure 4
tpIs15	*tpIs15[P_{ced-9m}::gfp]*	Figure 4
tpIs11	*tpIs11[P_{dre-1}::gfp]*	Figure 6
tpIs16	*tpIs16[P_{ced-3}::gfp]*	Figure S1